Journal of Materials Chemistry B

Accepted Manuscript

ROYAL SOCIETY OF CHEMISTRY

www.rsc.org/materialsB

Redox-responsive nanoreservoirs based on collagen end-capped mesoporous hydroxyapatite nanoparticles for targeted drug delivery

Dalong Li,[a] Jinmei He,[a] Weilu Cheng,[a] Yadong Wu,[a] Zhen Hu,[a] Huayu Tian[b] and Yudong Huang*[ac]

[a] *School of Chemical Engineering and Technology, Harbin Institute of Technology, Harbin, 150001, P R China*

[b] *Changchun Institute of Applied Chemistry, Chinese Academy of Sciences, Changchun, 130022, P R China*

[c] *State Key Laboratory of Urban Water Resource and Environment, Harbin Institute of Technology, Harbin, 150001, P R China*

The corresponding author: Yudong Huang

Postal address:

School of Chemical Engineering and Technology,

State Key Laboratory of Urban Water Resource and Environment,

Harbin Institute of Technology,

Harbin, 150001,

P. R. China

E-mail: 12B925006@hit.edu.cn

Tel: +86-451-86414806

Fax: +86-451-86414806

* Corresponding author. Tel.:+86-451-86414806; Fax: +86-451-86414806
E-mail address: 12B925006@hit.edu.cn (Yudong Huang)

Redox-responsive nanoreservoirs based on collagen end-capped mesoporous hydroxyapatite nanoparticles for targeted drug delivery

Dalong Li,[a] Jinmei He,[a] Weilu Cheng,[a] Yadong Wu,[a] Zhen Hu,[a] Huayu Tian[b] and Yudong Huang*[ac]

[a] *School of Chemical Engineering and Technology, Harbin Institute of Technology, Harbin, 150001, P R China*

[b] *Changchun Institute of Applied Chemistry, Chinese Academy of Sciences, Changchun, 130022, P R China*

[c] *State Key Laboratory of Urban Water Resource and Environment, Harbin Institute of Technology, Harbin, 150001, P R China*

Abstract:

Mesoporous Hydroxyapatite (MHAp) nanoparticles have great potential in nanoscaled delivery devices due to excellent biocompatibility, nontoxicity and high surface areas. In order to achieve targeting based on cell-specific recognition and site pointed, timed and quantitatively controlled drug release to malignant cells, redox-responsive nanoreservoirs based on MHAp (LA-Col-S-S-MHAp) was fabricated by using lactobionic acid-conjugated collagen (LA-Col) as cap, disulfide bonds as intermediate linkers and MHAp as nanoreservior. Lactobionic acid (LA) molecules acted as targeting moiety to achieve the targeted drug delivery. The results of scanning electron microscope (SEM), transmission electron microscopy (TEM), Brunauer-Emmett-Teller (BET), Barett-Joyner-Halenda (BJH), Fourier transform infrared spectroscopy (FTIR) and zeta potential measurements confirmed the successful preparation of LA-Col-S-S-MHAp step-by-step. Dithiothreitol (DTT) was used as external stimulus to trigger the redox-responsive release of drug in order to investigate the controlled release behavior of LA-Col-S-S-MHAp. The result proved that LA-Col-S-S-MHAp nanocomposite has a good end-capping efficiency to drug under physiological conditions, whereas it has a characteristic of rapid response

* Corresponding author. Tel.:+86-451-86414806; Fax: +86-451-86414806
E-mail address: 12B925006@hit.edu.cn (Yudong Huang)

and burst drug release when exposed to reducing conditions. Confocal laser scanning microscopy (CLSM) images and flow cytometry assay demonstrated that LA-Col-S-S-MHAp nanoparticles were endocytosed and located in the cytoplasm of cells. Redox-responsive targeted drug delivery could be achieved within cells. The system affords references and ideas for designing novel stimuli responsive nanoreservoir to the clinical therapy of liver cancer.

1 Introduction

The construction of stimuli-responsive controlled-release systems for targeted drug delivery to specific cells is of crucial importance for the development of both fundamental science and clinical medicine. During the past decade, mesoporous materials have attracted much attention because of their unique surface and textural properties such as high surface areas, small, tunable pore sizes, and large pore volumes, which are crucial for developing new types of catalysts, sorbents, drug carriers and so on.[1-4] Due to the characteristics of mesoporous materials, it has become a hot topic in the field of biomedical applications, especially drug delivery device.[5,6] As effective drug carrier, drug-loaded nanoparticles should have excellent biocompatibility, biodegradability, subcellular size and high drug loading capacity.[7] For many drug-loaded system applications, "zero premature release" and "targeted controlled release" of the precious and often toxic pharmaceutical are two important prerequisites that would impact the therapeutic efficacy and cytotoxicity of drug delivery.[8,9] In recent years, mesoporous silica is the most widely application mesoporous materials. Mesoporous silica materials have been considered to be excellent candidates as carriers for drug delivery. On one hand, textural properties of mesoporous silica increase the loading amount of drugs by hosting them within pore channels. On the other hand, the silanol containing surface can be easily functionalized, allowing for a better control over the drug diffusion kinetics.[10] In the case of the functionalized mesoporous silica nanoparticles-based system, various molecules have been

demonstrated for stimuli responsive drug delivery, such as CdSe, Au, polyetherimide, gelatin, DNA and so on.[11-14] Although mesoporous silica materials have achieved some good results,[15,16] the overuse of silica may cause side effects such as cell mutation, chronic bronchitis even pulmonary cancer.[17] So it remains a big challenge to construct a smart controlled-release system for intracellular drug delivery in the field.

Hydroxyapatite [$Ca_{10}(PO_4)_6(OH)_2$] (HAp), which is the major inorganic component of bone and teeth, is a key biomaterial because of its excellent biocompatibility, bioactivity, and osteocoductivity.[18,19] Hydroxyapatite (HAp) has gained much attention in recent years due to its potential applications in several fields such as in orthopedic, drug carriers, bioceramic industry, pharmaceutical areas and in environmental pollution control.[20,21] HAp has achieved excellent results as bioceramics in bone substituted operations and teeth repair due to its unique mechanical properties and bioactivity.[22,23] Moreover, owing to its nontoxicity and noninflammatory properties, it has great potential application in drug storage/release system.[24] As effective drug carrier, high drug loading capacity is necessary.[25,26] But the low surface area of HAp may limit its further application in many conditions. Therefore, synthesis of functionalized mesoporous hydroxyapatite (MHAp) with nano-sized and large pore volumes should be able to reach this goal.[27-29] Currently, mesoporous HAp with various morphology and surface properties has been investigated as a nanocarriers due to its biocompatible and osteoconductive properties; solubility and less toxicity than silica, quantum dots, carbon nanotubes.[30-32] Yang and coworkers reported the design and development of luminescent HAp mesoporous nanoparticles with a high loading for ibuprofen (over 40 wt. %), though the carrier had uncontrolled release kinetics which made it have a burst release of ibuprofen of over 50% within 1 h.[33] In addition, many functionalized mesoporous HAp was also used to control release and targeted drug delivery, for example carboxylic acid and sulfonic acid have been modified on the surface of HAp to further improve their surface property.[34-38] Nevertheless, none of these reports combined end-capped MHAp and

cell-specific targeting for stimuli-responsive controlled drug release.

Therefore, we prepare nanoreservoirs based on mesoporous HAp that are end-capped with collagen and demonstrate great potential for both cell targeting and redox-responsive controlled drug release. Collagen, which is one of extracellular matrix (ECM) components, was employed as a cap to encapsulate fluorescent probes within the porous channels of the MHAp. Collagen was immobilized on the exterior surfaces of the MHAp by disulfide bonds, which can be cleaved with various reducing agents, such as dithiothreitol (DTT).[39-41] Thus, we could achieve redox-responsive controlled drug release from an end-capped MHAp system. Lactobionic acid (LA), which bears a galactose group, was introduced as the targeting moiety.[42] This is the first study in which the collagen is employed with an auxiliary carrier to construct a redox-responsive controlled release system based on MHAp for targeted drug delivery. We hypothesized that the end-capped MHAp could serve as a nanoreservoir for a redox-responsive controlled release system for targeted drug delivery.

2 Materials and Methods

2.1 Materials

Pluronic F127, 1-[3-(Dimethylamino)propyl]-3-ethylcarbodiimide hydrochloride, N-hydroxysuccinimide, fluorescein isothiocyanate, lactose acid and dithiothreitol were purchased from Sigma Chemical Co. (St. Louis, MO, USA). Calcium pantothenate, hydrogenphosphate trihydrate, 3-aminopropyltriethoxysilane, cystaminedihydrochloride, succinic anhydride, trypan blue and triton X-100 were obtained from J&K Scientific Co. (BeiJing, PR China). HepaG2 cells, endothelial cells, bovine serum, penicillin and streptomycin were provided by Sanggon biotech Co. (Shanghai, PR China). Type Ⅰ collagen was prepared from our laboratory. All the initial chemicals in the work were used without further purification.

2.2 Preparation of mesoporous Hydroxyapatite (MHAp)

The mesoporous HAp nanoparticles were synthesized using the templating method based on a modified method in the literature.[43,44] Block co-polymer pluronic F127 (EO99PO65EO99) was selected as template. Firstly, 3.5 g of F127 and 19.33 g of calcium pantothenate ($C_{18}H_{32}CaN_2O_{10}$) were co-dissolved in 150 g of distilled water to form solution 1. Then, 5.60 g of potassium hydrogenphosphate trihydrate ($K_2HPO_4 \cdot 3H_2O$) was dissolved in 60 g of distilled water to form solution 2. Solution 1 was stirred for 1 h at 37 ℃. The pH of solution 2 was adjusted to 12 with ammonia (NH_3H_2O). Finally, solution 2 was added dropwise to solution 1. The mixture solution was heated to 90 ℃ under reflux for 24 h and filtered to get precipitate. The white precipitate was then calcined at 600 ℃ for 6 h.

2.3 Preparation of disulfide bonds functionalized MHAp (S-S-MHAp)

Firstly, 1.42 g of MHAp and 7.5 ml of 3-aminopropyltriethoxysilane were dissolved in 80 ml toluene under stirring condition. The mixture solution was heated to 60 ℃ under reflux for 36 h and filtered to get NH_2-MHAp by vacuum drying. Then, 1.1 g of NH_2-MHAp was dissolved in 80 ml of acetone under slowly stirring. 7.62 g of succinic anhydride (SA) was added to the solution and vigorous stirring was continued. The solution was filtered after 48 h. The precipitate was eluted with ethanol and water six times to remove solvent. COOH-MHAp was obtained after dry.[42] Finally, 0.62 g of COOH-MHAp, 1.15 g of N-hydroxysuccinimide (NHS) and 0.35 g of 1-[3-(Dimethylamino)propyl]-3-ethylcarbodiimide hydrochloride (EDC) were co-dissolved in 60 ml pH 5.0 PBS solution and stirred for 3 h. 6.0 g of cystaminedihydrochloride (Cys) was added to above solution, and mixture solution was continuously stirred for 36 h under 25 ℃. The solution was centrifuged after the reaction completed. The obtained precipitate was washed with ethanol and water ten times. Finally the product was dried in an vacuum oven at 100 ℃ for 12 h to get S-S-MHAp.

2.4 The construction of lactose acid (LA) functionalized redox-responsive MHAp/collagen systems

(LA-Col-S-S-MHAp/FITC)

Fluorescein isothiocyanate (FITC) was utilized as both model drug and site marker for intracellular tracing of MHAp. The S-S-MHAp/FITC was further covalently coupled with collagen to attach the FITC-loaded mesopores to the MHAp. Firstly, 0.0596 g of FITC and 0.30 g of S-S-MHAp were dissolved in 30 ml pH 6.0 PBS solutions and stirred for 24 h. Then 25 mg of collagen was added to the above mixture solution and continuously stirred 36 h. By reaction of carboxyl groups of collagen and amino groups of S-S-MHAp, redox-responsive MHAp nanoreservoirs end-capped with collagen was constructed. Finally, 100 mg of Lactose acid (LA) was added to the collagen-capped MHAp solution and stirred for 24 h. The mixture solution was centrifuged and eluted with ethanol and water ten times to remove unencapsulated FITC. Cell-specific targeting moiety LA-Col-S-S-MHAp/FITC was constructed after vacuum freeze-dried 36 h (Fig. 1).

2.5 Preparation of Col/MHAp-FITC

In the control group, collagen was physically coated on the surface of MHAp (Col/MHAp). 0.0596 g of FITC and 0.35 g of MHAp were dissolved in 30 ml pH 6.0 PBS solutions and stirred for 24 h. Then 30 mg of collagen was added to the above mixture solution and continuously stirred 36 h. The mixture solution was centrifuged and eluted with ethanol and water six times to remove unencapsulated FITC. Finally the solution was vacuum freeze-dried for 24 h to get physical coating of Col/MHAp-FITC.

2.6 Drug load and release assay

The LA-Col-S-S-MHAp was used as carrier for FITC. End-capping efficiency and release behavior of LA-Col-S-S-MHAp/FITC were detected by UV-vis fluorescence spectroscopy. 3.3 mg of LA-Col-S-S-MHAp/FITC and 5 mg of DTT were incubated in PBS (3 ml, pH 7.2) at 37 ℃ for 24 h to as solution 1. 3.3 mg of LA-Col-S-S-MHAp/FITC and 3.3 mg of Col/MHAP-FITC (collagen was physically coated on the

surface of MHAp) were incubated in PBS (3 ml, pH 7.2) at 37 ℃ for 24 h to as solution 2 and 3, respectively. The release amount of FITC each group in the PBS solution was measured by UV-vis fluorescence spectroscopy at every 1 h. Another assay, 3.3 mg of LA-Col-S-S-MHAp/FITC was incubated in PBS (3 ml, pH 7.2) at 37 ℃ for 5 h. Then 5 mg of DTT was added to co-incubate for 24 h. The release amount of FITC was measured by UV-vis fluorescence spectroscopy at every 1 h. The curve of UV-vis fluorescence spectroscopy reflects the end-capping efficiency and release behavior of LA-Col-S-S-MHAp/FITC system.

2.7 Cell culture

HepaG2 cells and endothelial cells were cultured in low-glucose Dulbecco's Modified Eagle's Medium supplemented with 10% bovine serum (FBS; Gibco), 100 U/ml of penicillin and 100 ug/ml of streptomycin at 37 ℃ under a 5% CO_2 atmosphere, respectively. Cell culture media was changed every 2 days. When reaching confluence, cells were detached with 0.25% trypsin in 1 mM tetrasodium EDTA, centrifuged and resuspended in complete medium for reseeding in new culture flasks.

2.8 Confocal laser scanning microscopy (CLSM) observation

HepaG2 cells were cultured on 24-well plates at an initial density of 2×10^4 cells cm^2. After 7 days, 20 ug/ml of LA-Col-S-S-MHAp/FITC was added to co-incubate. After culture 4 h and 8 h, 200 ug/ml of trypan blue was added to quench fluorescence of extracellular for 10 min, respectively. After cells were fixed with 2% glutaraldehyde at 4 ℃ for 20 min, the fixed samples were then rinsed with excessive PBS buffer and permeabilized with 0.2% Triton X-100 at 4 ℃ for 10 min. The nuclei of cells were stained with 10 ug/ml of Hoechst 33258 at 4 ℃ for 10 min. Finally, the stained samples were mounted with 90% glycerine. The distributions of fluorescently labeled nanoparticles in HepaG2 cells was observed with confocal laser scanning microscopy (CLSM).

2.9 Flow cytometry

The number of HepaG2 cells and endothelial cells, which engulfed MHAp and LA-Col-S-S-MHAp, was detected by flow cytometry. HepaG2 cells and endothelial cells were cultured on 24-well plates at an initial density of 2×10^4 cells cm^2, respectively. After 7 days, 20 ug/ml of MHAp/FITC and LA-Col-S-S-MHAp/FITC were added to co-incubate. After culture 4 h and 8 h, 200 ug/ml of trypan blue was added to quench fluorescence of extracellular for 10 min, respectively. Cells were then rinsed with excessive PBS buffer. Cells were then analyzed with BD FACS Aria.

2.10 Characterization

A series of characterization technique was used to analyze the structural properties of each product. The nanoparticles morphology and mesoporous aperture of the sample were observed by scanning electron microscopy (SEM; Hitachi4700) and transmission electron microscopy (TEM; Philips EM20). The structure of MHAp and functionalized MHAp was analyzed by Fourier transform infrared (FTIR; VECTOR22, BRUKER) spectrum within the scanning range of 4000-400 cm^{-1} using the KBr pellet technique. N_2 adsorption-desorption isotherms was measured with an automatic surface area and porosity analyzer (3H-2000PS2, Beishide) at 77 K. The specific surface area was determined by the Brunauer-Emmett-Teller (BET) method using the date between 0.03 and 0.95. The pore-size distributions was derived from the desorption branches of the isotherms using the Barrett-Joyner-Halanda (BJH) method. The charge property of each product was analyzed using zeta potential (Nanotrac wave, Microtrac). Control release property of the drug was detected by UV-vis fluorescence spectrophotometer (LS50B, PerkinElmer). Confocal laser scanning microscopy (CLSM, LSM 510Metanlo, Zeiss) was used to detect the distribution of the fluorescence-drug within the cells. The result of drug targeting delivery was conformed using the Flow cytometry (Becton Dickinson).

3 Results and Discussion

Fig. 1 shows a schematic of the construction of redox-responsive nanoreservoirs based on collagen-capped mesoporous hydyoxyapatite (MHAp) for cell targeted drug delivery. MHAp was synthesized using the templating method. MHAp nanoreservoirs was loaded with model drug FITC and then grafted with collagen by disulfide bonds. Along with the breakage of disulfide bonds under redox environments, loaded FITC would be released to specific cells. Collagen has good biocompatibility and was introduced to end-cap the nanoreservoirs and improve its biological efficiency.

Insert Fig. 1 here

3.1 SEM and TEM images

Mesoporous HAp (MHAp) nanoparticles were synthesized through a templating method using F123 micelle.[43] Fig. 2a and b show the SEM micrographs of MHAp and LA-Col-S-S-MHAp, respectively. It can be seen that MHAp and LA-Col-S-S-MHAp show nanospheres distribution with average diameter of around 100 nm and 120 nm (Fig. 2a and b). Because of grafting collagen, diameter of LA-Col-S-S-MHAp becomes large. TEM observations were carried out to verify the existence of mesoporoes aperture and confirm the pore size. The TEM micrographs of MHAp are shown in Fig. 2c. Mesoporous structure was confirmed to exist in this sample, and the lattice array over the MHAp indicated an irregular mesostructure with an average pore size of 4.3 nm (Fig. 2c). Fig. 2d shows the TEM picture of sample LA-Col-S-S-MHAp. Without significantly pore structure, a border was observed around the LA-Col-S-S-MHAp. The main reason is that collagen has endcapped the mesoporous aperture of MHAp (Fig. 2d). So the result of SEM and TEM shows that mesoporous HAp has been successfully synthesized, and well encapsulated by collagen.

Insert Fig. 2 here

3.2 FTIR analysis

The FT-IR spectra of MHAp (a), NH_2-MHAp (b), COOH-MHAp (c), S-S-MHAp (d), Col-S-S-MHAp (e) and LA-Col-S-S-MHAp (f) are shown in Fig. 3, respectively. The intense absorption peak at 1030 cm^{-1} is ascribed to the stretching vibration of the phosphate (PO_4^{3-}) groups, and the absorption peaks at 563 and 608 cm^{-1} belong to the bending vibration of the phosphate (PO_4^{3-}) groups of hydroxyapatite (Fig. 3a).[44,45] The weak bands at 3400 cm^{-1} are assigned to OH^- group. It is caused one with OH^- group hydrogen bonded with phosphate group and other one with weak interactions to the environments. The band appears at 1563 cm^{-1} attributed to the N-H stretching vibrations of NH_2-MHAp (Fig. 3b). So amino groups have been grafted the surface of MHAp. The bands at 1713 cm^{-1} belong to C-O stretching vibrations of COOH-MHAp (Fig. 3c), and absorption intensity of 1563 cm^{-1} became weaken. The result shows the carboxyl groups have replaced amino groups. In Fig. 3d, the peak of 1563 cm^{-1} is ascribed to the N-H stretching vibrations of -S-S-MHAp. After collagen was grafted onto MHAp, 1659 cm^{-1} and 1552 cm^{-1} appeared obvious absorption peaks (Fig. 3e). It assigned to the C=O stretching vibrations and C-N bending vibrations of collagen, respectively. Previous studies have confirmed the absorption peaks of C=O and C-N will move to low after collagen graft lactose acid.[46] In Fig. 3f the C=O stretching vibrations change from 1659 cm^{-1} to 1617 cm^{-1}. So lactose acid was introduced. These results suggest the disulfide bonds, collagen, lactose acid have been successfully grafted to the surface of mesoporous HAp nanoparticles.

Insert Fig. 3 here

3.3 BET and BJH analysis

The respective N_2 adsorption/desorption isotherms of MHAp and LA-Col-S-S-MHAp are shown in Fig. 4. The Brunauer-Emmett-Teller (BET) surface area and pore volume of MHAp are 76.60 m^2g^{-1} and 0.26 cm^3g^{-1}, respectively, and the pore size distribution is between 3-5 nm, in agreement with the TEM observation. The

textural parameters of the corresponding materials are summarized in Table 1. It can be seen mesoporous HAp shows typical H_1-hysteresis loops, demonstrating the properties of typical mesoporous materials. When the mesopores of the MHAp were sealed by collagen molecules, surface area of the MHAp sharply decreased from 76.60 m^2g^{-1} to 1.14 m^2g^{-1}. The BET pore volume and BJH pore diameter didn't be detected after grafting collagens molecules. N_2 adsorption/desorption isotherms of LA-Col-S-S-MHAp didn't also shown mesoporous characteristic. The reason is that N_2 can't enter into mesoporous aperture of MHAp encapsulated by collagen, so pore volume and pore size can not be detected.[47] The result demonstrated that LA-Col-S-S-MHAp has been successfully prepared.

Insert Table 1 here

Insert Fig. 4 here

3.4 Zeta potential measurement

A zeta potential measurement is also used to characterize the LA-Col-S-S-MHAp. Zeta potential value of MHAp exhibits strongly negative (-25.53). Potential value of aminated mesoporous HAp (NH_2-MHAp) is 15.56, because amino groups absorbed positive charge H^+. COOH can dissociate H^+, so COOH-MHAp shows negative potential value (-18.6). Since both the positive charge of collagen and negative charge of MHAp reaction, Col-S-S-MHAp appears eletroneutralityl (0.096). The corresponding data is shown in Table 2. The zeta potential measurements further confirmed the functional groups were successfully introduced.

Insert Table 2 here

3.5 Drug load and release properties

In order to research the controlled release behavior of LA-Col-S-S-MHAp syetem, dithiothreitol (DTT) was used as external stimulus to trigger the redox-responsive release of FITC. The about 20% of FITC was released

from LA-Col-S-S-MHAp within 10 hours without DTT, thus the composite system indicates a good end-capping efficiency (Fig. 5A, a). The leakage reason of FITC may be partial physical degradation of end-capping collagen molecules when without DTT stimulate. However, LA-Col-S-S-MHAp/FITC system exhibited 80% release within 10 hours after addition of DTT, thus the system shows a rapid response to DTT (Fig. 5A, c). This reason attribute to the disulfide linkages between collagen and MHAp were broken, thus leading to a redox response to DTT. At the same time, collagen was physically coated on the surface of MHAp (Col/MHAp-FITC) rather than by disulfide bonds to study end-capping efficiency and response. Fig. 5A b shows Col/MHAp-FITC exhibited around 80% FITC leaching after 20 h, however only 25% of FITC was released from LA-Col-S-S-MHAp after 20 h when without DTT (Fig. 5A, a). The result could be interpreted that physically coated Col/MHAp system have not a good end-capping efficiency to compare to disulfide linkages Col-S-S-MHAp. To further investigate the rapid redox response of LA-Col-S-S-MHAp to reducing agent stimulus, DTT was added to the solution after LA-Col-S-S-MHAp/FITC was cultivated in PBS buffer solution for 5 hours. The result shows when without DTT about 10% of FITC was released after the first 5 hours, whereas along with DTT addition, 70% of FITC was released after a subsequent 5 hour. The release of FITC could be clearly visualized from the color change of solution (Fig. 5B). The phenomenon further demonstrated disulfide linkages between collagen and MHAp have a redox-response to DTT. Taken together, the LA-Col-S-S-MHAp/FITC nanocomposite has a good end-capping efficiency to drug under physiological conditions, whereas it has a characteristic of rapid response and burst drug release when exposed to reducing conditions.

Insert Fig. 5 here

3.6 Cell uptake

Confocal laser scanning microscopy (CLSM) was used to investigate the cell-uptake properties and

distribution of the model drug in the cell. LA-Col-S-S-MHAp/FITC was incubated with HepaG2 cells for 4 h and 8 h. CLSM imaging revealed when LA-Col-S-S-MHAp/FITC and HepaG2 cells were co-incubated 4 h, the cytoplasm of HepaG2 cells appeared small amounts fluorescent particles (Fig. 6a). With time prolonged, fluorescent particles of cytoplasm significantly increased after 8 h (Fig. 6b). The result indicates that LA-Col-S-S-MHAp/FITC can sustainable militate with HepaG2 cells and can continue to be cell-uptake. LA-Col-S-S-MHAp/FITC nanoparticles showed superior cell-uptake properties. After LA-Col-S-S-MHAp/FITC was engulfed, the model drug FITC would be released. The result once again demonstrated LA-Col-S-S-MHAp was good cytocompatible for drug carrier and can be used in vivo drug delivery. If anti-drugs were applied to the LA-Col-S-S-MHAp materials in clinical, it has potential to overcome the problem of cancer.

Insert Fig. 6 here

The endocytosis efficiency was quantified by flow cytometry. LA-Col-S-S-MHAp/FITC and MHAp/FITC (no capping) were incubated with HepaG2 cells for 4 h and 8 h, respectively. LA-Col-S-S-MHAp/FITC nanoparticles display excellent cell-uptake properties compared to MHAp/FITC. LA-Col-S-S-MHAp/FITC shows endocytosis efficiencies that are about 2.5 times higher after 4 h and 2.4 times higher after 8 h, than that of MHAp/FITC (Fig. 7a). The result further suggests that lactose acid functioned Col-S-S-MHAp was easier endocytosed than MHAp, which has potential to be an excellent drug carrier.

To confirm the potential of LA-Col-S-S-MHAp has a targeting drug delivery, we further demonstrated the endocytosis and intracellular delivery of nanoparticles by HepaG2 cells and endothelial cells (EC). Because surface of HepaG2 cells has a large number ligand of lactobionic acid, it is easier to endocytose lactose acid functioned Col-S-S-MHAp than other cell in theory. Interestingly, Fig. 7b displays that endocytosis number of HepaG2 cells that internalized LA-Col-S-S-MHAp was 2.2 and 2 times higher than that of endothelial cells after

incubation for 4 h and 8 h, respectively. This result demonstrates the targeting property of LA-Col-S-S-MHAp to HepaG2 cells. The targeting mechanism could be interpreted that specific ligand-asialoglycoprotein receptor (ASGP-R) of lactobionic acid exist on the membrane of HepaG2 cells, which the galactose groups on LA-Col-S-S-MHAp can specific recognize.[49,50] Overall, we confirmed our hypothesis that collagen-capped MHAp could serve as nanoreservoirs in a redox-responsive controlled release system for targeted drug delivery.

Insert Fig. 7 here

4 Conclusion

In this study, mesoporous hydroxyapatite nanoparticles were successfully synthesized, and SEM, TEM proved the presence of mesoporous. The surface of MHAp nanoparticles was successfully end-capped with collagen. The LA-Col-S-S-MHAp system was confirmed by FTIR absorption spectra, BET, BJH and Zeta potential. We have also successfully demonstrated that collagen-capped mesoporous HAp nanoparticles could serve as a redox-responsive nanoreservoir for efficient targeted drug delivery to cancer cells. LA-Col-S-S-MHAp composites achieve not only targeting based on cell-specific recognition, but also site pointed, timed and quantitatively controlled drug release to malignant cells via a "biological explosion" approach. More importantly, the excellent biocompatibility, nontoxicity and noninflammatory properties of MHAp nanoparticles outline the great potential for future biomedical applications that require in vivo controlled, targeted drug delivery. The system provides a new way of thinking for the clinical therapy of liver cancer.

Acknowledgements

This work was financially supported by Shandong Province Postdoctoral Foundation of China (201101003), Fundamental Research Funds for the Central Univesities (HIT. NSRIF2015047), and Weihai Science and Technology Development Plan project (2013GNS028) from Weihai city, Shandong province of China.

References

1 M. E. Davis, *Nature*, 2002, **417**, 813-821.

2 A. Dong, N. Ren, Y. Tang, Y. Wang, Y. Zhang, W. Hua and Z. Gao, *J. Am. Chem. Soc.*, 2003, **125**, 4976-4977.

3 N. T. Chen, S. H. Cheng, J. S. Souris, C. T. Chen, C. Y. Mou and L. W. Lo, *J. Mater. Chem. B*, 2013, **1**, 3128-3135.

4 D. M. Antonelli and J. Y. Ying, *Angew. Chem., Int. Ed.*, 1996, **35**, 426-430.

5 N. Singh, A. Karambelar, L. Gu, K. Lin, J. S. Milier, C.S. Chen, M. J. Sailor and S. N. Bhatia, *J. Am. Chem. Soc.*, 2011, **133**, 19582-19585.

6 S. R. Choi, D. J. Jang, S. Kim, S. An, J. Lee, E Oh and J. Kim, *J. Mater. Chem. B*, 2014, **2**, 616-619.

7 K. E. Uhrich, S. M. Cannizzaro, R. S. Langer and K. M. Shakesheff, *Chem. Rev.*, 1999, **99**, 3181-3198.

8 S. Dekoker, R. Hoogenboom and B. G. Degeest, *Chem. Soc. Rev.*, 2012, **41**, 2867-2884.

9 S. L. Zhang, Z. Q. Chu, C. Yin, C. Y. Zhang, G. Lin and Q. Li, *J. Am. Chem. Soc.*, 2013, **135**, 5709-5716.

10 F. Balas, M. Manzano and M. Horcajada. *J. Am. Chem. Soc.*, 2006, **128**, 8116-8117.

11 R. A. Pai, R. Humayun, M. T. Schulberg, A. Sengupta, J. N. Sun and J. J. Watkins, *Science*, 2004, **303**, 507-510.

12 A. B. Descalzo, R. Martinez-Manez, R. Sancenon, K. Hoffmann and K. Rurack, *Angew. Chem., Int. Ed.*, 2006, **45**, 5924-5948.

13 N. K. Mal, M. Fujiwara and Y. Tanaka, *Nature*, 2003, **421**, 350-353.

14 Z. H. Li, Z. Liu, M. L. Yin, X. J. Yang, Q. H. Yuan, J. S. Ren and X. G. Qu, *Biomacromolecules*, 2012, **13**, 4257-4263.

15 L. M. Pan, Q. J. He, J. N. Liu, Y. Chen, M. Ma, L. L. Zhang and J. L. Shi, *J. Am. Chem. Soc.*, 2012, **134**, 5722-5725.'

16 E. Climent, M.R. Martinez, F. Sancenon, M. D. Marcos, J. Soto, A. Maquieira and P. Amoros, *Angew. Chem., Int. Ed.*, 2010, **49**, 7281-7283.

17 R. Merget, T. Bauer, H. U. Kupper, S. Philippou, H. D. Bauer, R. Breitstadt and T. Bruening, *Arch. Toxicol.*, 2002, **75**, 625-634.

18 S. S. Sandra, C. Montserrat, I. B. Isable and V. R. Maria, *J. Mater. Chem. B*, 2013, **1**, 1595-1606.

19 M. Li. Y. B. Wang, Q. Liu, Q. H. Li, Y. Cheng, Y. F. Zheng, T. F. Xi and S. C. Wei, *J. Mater. Chem. B*, 2013, **1**, 475-484.

20 J. Xu, T. White, P. Li, C. H. He and Y. F. Han, *J. Am. Chem. Soc.*, 2010, **132**, 13172-13173.

21 Y. F. Zhu, F. J. Shang, B. Li, Y. Dong, Y. F. Liu, M. R. Lohe, M. Hanagata and S Kaskel, *J. Mater. Chem. B*, 2013, **1**, 1279-1288.

22 L. A. Capriotti, T. P. Beebe and J. P. Schneider, *J. Am. Chem. Soc.*, 2007, **129**, 5281-5287.

23 H. J. Zhou and J. Lee, *Acta Biomater*, 2011, **7**, 2769-2781.

24 C. Zhang, C. Li, S. Huang, Z. Hou, Z. Cheng, P. Yang, C. Peng and J. Lin, *Biomaterials*, 2010, **31**, 3374-3383.

25 E. Climent, A. Bernardos, M. R. Martinea, A. Maquieira, M. D. Marcos, N. N. Pastor and R. Puchades, *J. Am. Chem. Soc.*, 2009, **131**, 14075-14080.

26 R. Jurgons, C. Seliger, A. Hilpert, L. Trahms, S. Odenbach and C. J. Alexiou, *Phys. Condens. Matter.*, 2006, **18**, 2893-2902.

27 H. M. Lin, H. Y. Lin and M. H. Chan, *J. Mater. Chem. B*, 2013, **1**, 6147-6156.

28 Y. P. Guo, Y. B. Yao, Y. J. Guo and C. Q. Ning, *Microporous Mesoporous Mater.*, 2012, 15, 245-251.

29 R. X. Sun, K. Z. Chen and Y. P. Lu, *Mater Res Bull.*, 2009, **44,** 1939-1942.

30 T, Chen, M. I. Shukoor, R. W. Wang, Z. L. Zhao, Q. Yang, S. Bamrungsap, X. L. Xiong and W. H. Tan, *ACS Nano.*, 2011, **5,** 7866-7873.

31 J. S. Son, M. Appleford, J. L. Ong, J. C. Wenke, J. M. Kim and D. S. Oh, *J. Control. Release.,* 2011, **153,** 133-140.

32 F. Chen, P. Huang, Y. J. Zhu, J. Wu, C. L. Zhang and D. X. Cui, *Biomaterials*, 2011, **32,** 9031-9039.

33 P. P. Yang, Z. W. Quan, C. X. Li, X. J.Kang, H. Z. Lian and J. Lin, *Biomaterials*, 2008, **29,** 4341-4347.

34 X. Y. Yuan, B. S. Zhu, G. S. Tong, Y. Su and X. Y. Zhu, *J. Mater. Chem. B*, 2014, **1**, 6551-6559.

35 P. Nabakumar and I. Tokoko, *Langmuir*, 2012, **28,** 14018-14027.

36 E. M. Wassim, L. Danielle, G. Gilles, M. E. Smith and P. H. Mutin, *J. Mater. Chem.*, 2012, **22,** 1212-1218.

37 Y. H. Yang, C. H. Liu, F. H. Lin, Y. H. Liang and K. C. Wu. *J. Mater. Chem. B.*, 2013, **1,** 2447-2450.

38 Y. P. Guo, T. Long, S. Tang, Y. J. Guo and Z. A. Zhu, *J. Mater. Chem. B.*, 2014, **2,** 2899-2909.

39 R. Liu, X. Zhao, T. Wu and P. Y. Feng, *J. Am. Chem. Soc.*, 2008, **130,** 14418-14419.

40 Z. Luo, K. Y. Cai, Y. Hu, Z. Li, L. Peng, D. Lin and W. H. Yang, *Angew. Chem., Int. Ed.*, 2011, **50,** 640-643.

41 H. Kim, S. Kim, C. Y. Park, H. Lee, H. J. Park and C. Kim, *Adv. Mater.*, 2010, **22,** 4280-4283.

42 A. Bernardos, E. Aznar, M. D. Marcos, M. R. Martinez, F. Sancenon, J. Soto, J. M. Barat and P. Amoros, *Angew. Chem., Int. Ed.*, 2009, **48,** 5884-5887.

43 Y. H. Zhao and J. Ma, *Microporous Mesoporous Mater.*, 2005, **87,** 110-117.

44 J. Zhang, Q. Wang and A. Wang, *Acta Biomater.*, 2010, **6,** 445-454.

45 H. Takeda, Y. Seki, S. Nakamura and E. Yamashita, *J. Mater. Chem.*, 2002, **12,** 2490-2495.

46 R. Liu, Y. Zhang, X. Zhao, A. Agarwal, L. J. Mueller and P. Feng, *J. Am. Chem. Soc.*, 2010, **132,** 1500-1501.

47 B. J. Wu, Y. J. Zhu, S. W. Cao and F. Chen, *Adv. Mater.*, 2010, **22,** 749-753.

48 K. Y. Cai, Y. Hu, Z. Luo, T. Kong, M. Lai, X. Sui, Y. Wang and L. Deng, *Angew. Chem., Int. Ed.*, 2008, **47,** 7479-7481.

49 L. Du, S. Liao, H. A. Khatib, J. F. Stoddart and J. L. Zink, *J. Am. Chem. Soc.*, 2009, **131,** 15136-15142.

50 E. M. Kim, H. J. Jeong, S. L. Kim, J. W. Nah, H. S. Bom, I. K. Park and C. S. Cho, *Nucl. Med. Biol.*, 2006, **33,** 529-534.

Figure Captions:

Fig. 1 Schematic illustration of redox-responsive system based on collagen-capped MHAp for cell targeted drug delivery

Fig. 2 Fabrication of a nanoreservoir based on a redox-responsive MHAp for targeted drug delivery and cell uptake in situ. Scanning electron micrographs of MHAp (a, left) and LA-Col-S-S-MHAp (b, right). Transmission electron micrographs of MHAp (c, left) and LA-Col-S-S-MHAp (d, right)

Fig. 3 FTIR spectra of sample: (a) MHAp; (b) NH_2-MHAp; (c) COOH-MHAp; (d) S-S-MHAp; (e) Col-S-S-MHAp; (f) LA-Col-S-S-MHAp

Fig. 4 Nitrogen adsorption-desorption isotherm of MHAp and LA-Col-S-S-MHAp. The insets show BJH pore size distribution

Fig. 5 Cumulative release profiles of FITC from LA-Col-S-S-MHAp with/without DTT solution: A) controlled release of FITC from LA-Col-S-S-MHAp (a and b without DTT, c with DTT) and the Col/MHAp system (b); B) delayed release of FITC from LA-Col-S-S-MHAp by addition of DTT solution after incubation for 5 h

Fig. 6 Representative confocal microscopy images of LA-Col-S-S-MHAp/FITC endocytosed by HepaG2 cells for (a) 4 h, (b) 8 h

Fig. 7 (a) Quantification of endocytosis of MHAp/FITC without capping and LA-Col-S-S-MHAp/FITC and by HepaG2 cells; (b) flow cytometry analysis for specific endocytosis of LA-Col-S-S-MHAp/FITC by HepaG2 cells and endothelial cells

Table Captions

Table 1 Textural parameters of MHAp and LA-Col-S-S-MHAp

Table 2 Zeta potential results of MHAp before and after grafting with chemicals at each step

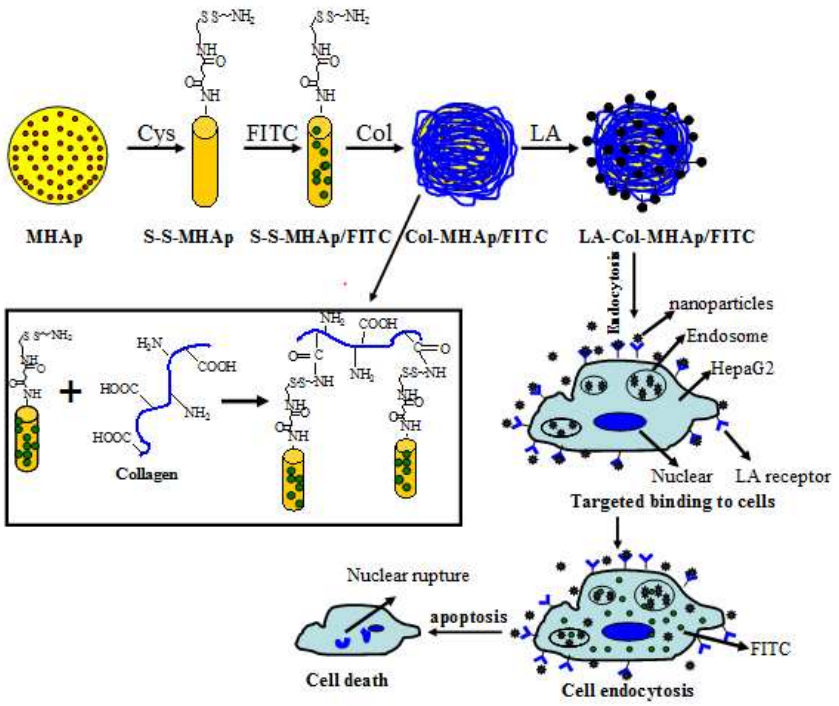

Dalong Li, et al. Fig. 1 Schematic illustration of redox-responsive system based on collagen-capped MHAp for cell targeted drug delivery

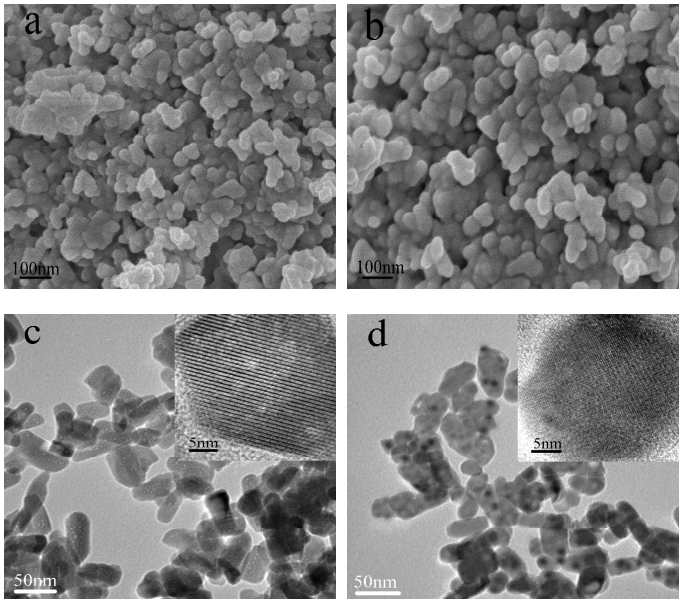

Dalong Li, et al. Fig. 2 Fabrication of a nanoreservoir based on a redox-responsive MHAp for targeted drug delivery and cell uptake in situ. Scanning electron micrographs of MHAp (a, left) and LA-Col-S-S-MHAp (b, right). Transmission electron micrographs of MHAp (c, left) and LA-Col-S-S-MHAp (d, right)

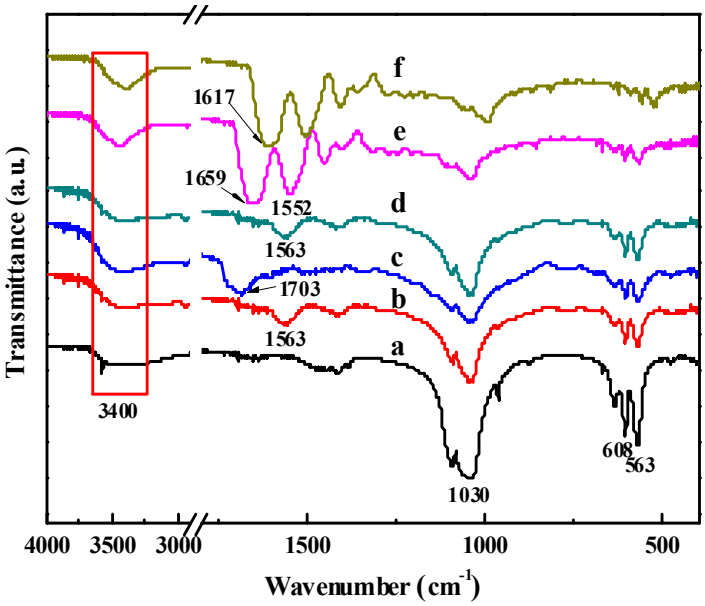

Dalong Li, et al. Fig. 3 FTIR spectra of sample: (a) MHAp; (b) NH_2-MHAp; (c) COOH-MHAp; (d) S-S-MHAp; (e) Col-S-S-MHAp; (f) LA-Col-S-S-MHAp

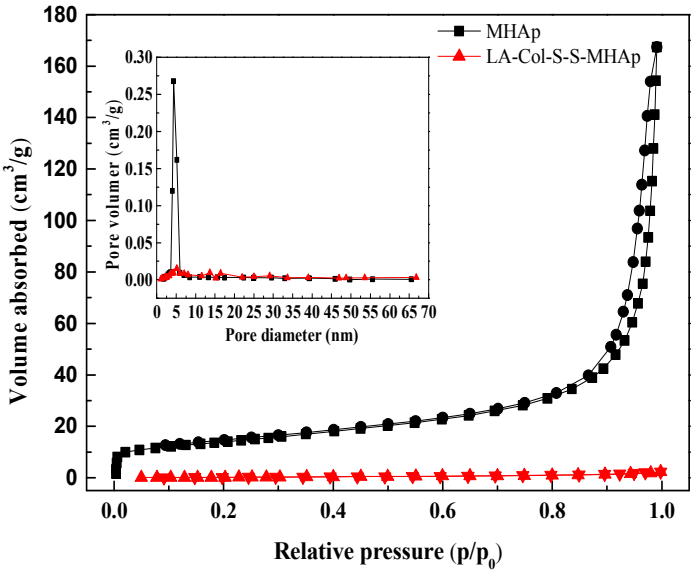

Dalong Li, et al. Fig. 4 Nitrogen adsorption-desorption isotherm of MHAp and LA-Col-S-S-MHAp. The insets show BJH pore size distribution

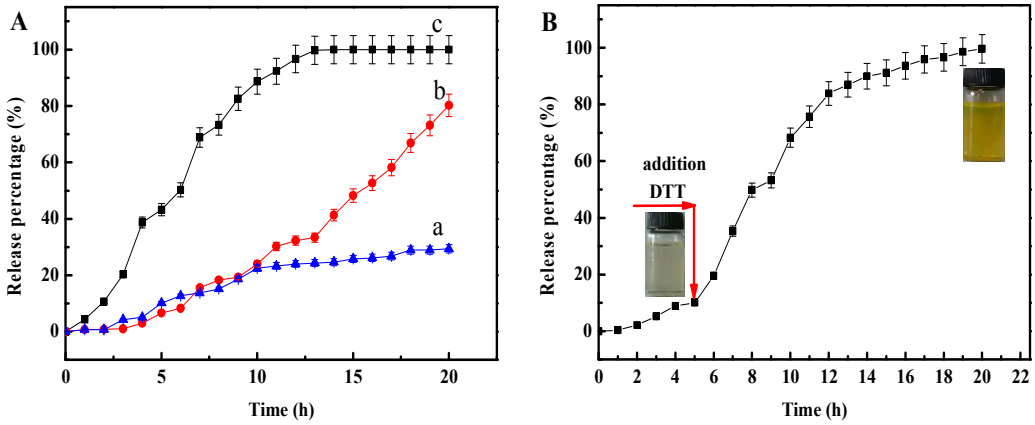

Dalong Li, et al. Fig. 5 Cumulative release profiles of FITC from LA-Col-S-S-MHAp with/without DTT solution: A) controlled release of FITC from LA-Col-S-S-MHAp (a and b without DTT, c with DTT) and the Col/MHAp system (b); B) delayed release of FITC from LA-Col-S-S-MHAp by addition of DTT solution after incubation for 5 h

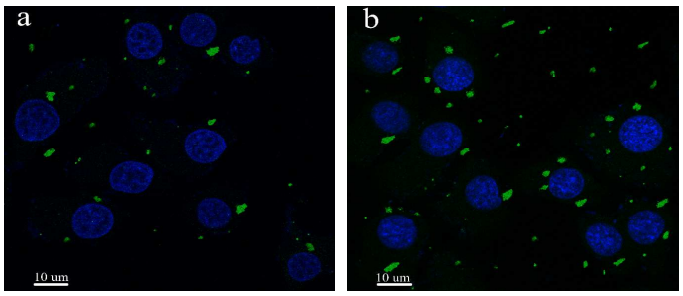

Dalong Li, et al. Fig. 6 Representative confocal microscopy images of LA-Col-S-S-MHAp/FITC endocytosed by HepaG2 cells for (a) 4 h, (b) 8 h

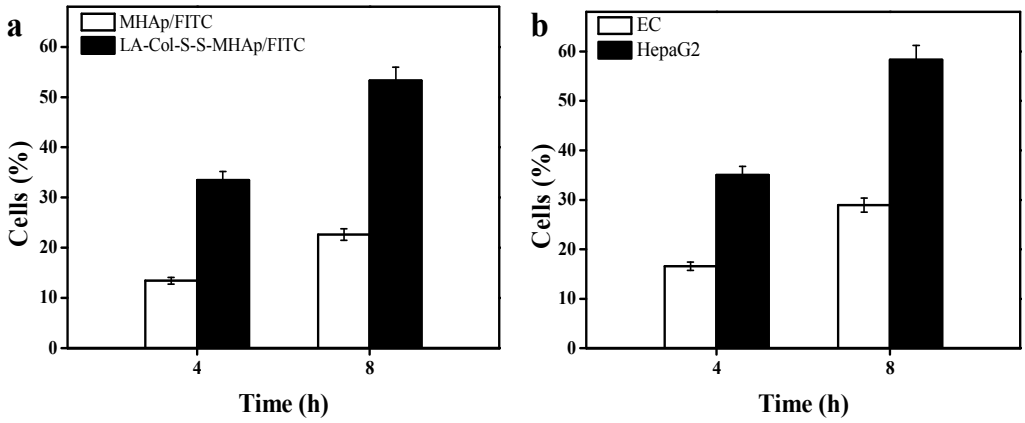

Dalong Li, et al. Fig. 7 (a) Quantification of endocytosis of MHAp/FITC without capping and LA-Col-S-S-MHAp/FITC and by HepaG2 cells; (b) flow cytometry analysis for specific endocytosis of LA-Col-S-S-MHAp/FITC by HepaG2 cells and endothelial cells

Dalong Li, et al. Table 1 Textural parameters of MHAp and LA-Col-S-S-MHAp

Samples	S_{BET} (m^2/g)	Vp (cm^3/g)	BJH (nm)
MHAp	76.60	0.260	4.32
NH_2-MHAp	74.56	0.198	3.96
S-S-MHAp	74.43	0.185	3.32
LA-Col-S-S-MHAp	1.14	-	-

Dalong Li, et al. Table 2 Zeta potential results of MHAp before and after grafting with chemicals at each step

Samples	Zeta potential (mv)
MHAp	-25.53
NH_2-MHAp	10.62
COOH-MHAp	-18.62
S-S-MHAp	15.56
Col-S-S-MHAp	-1.03
LA-Col-S-S-MHAp	-0.68

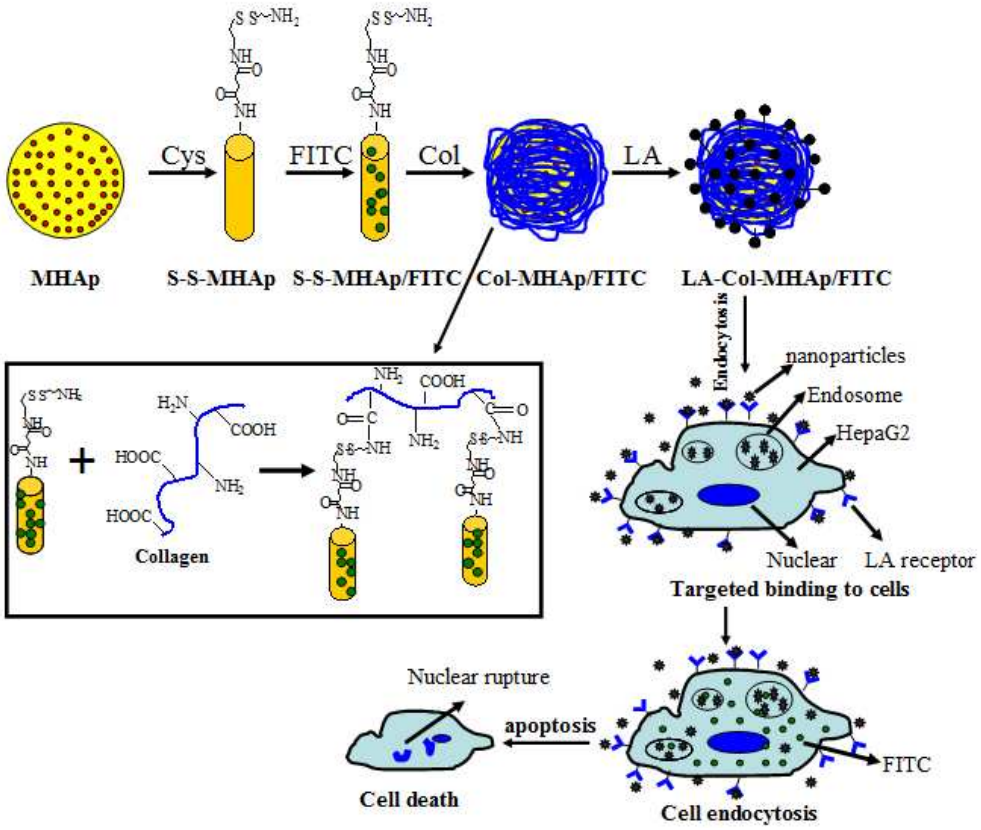

Dalong Li, et al. Graphical abstract.

Schematic illustration of redox-responsive system based on collagen-capped MHAp for cell targeted drug delivery